**Atmospheric
Chemistry
and Physics**

Sensitivity studies of the recent new data on $O(^1D)$ quantum yields in O_3 Hartley band photolysis in the stratosphere

N. Taniguchi[1], S. Hayashida[1], K. Takahashi[2], and Y. Matsumi[2]

[1]Faculty of Science, Nara Women's University, Kitauoya - Nishimachi, Nara, 630 - 8506, Japan
[2]Solar - Terrestrial Environment Laboratory, Nagoya University, Honohara 3 - 13, Toyokawa, 442 - 8507, Japan

Abstract. The production yields of excited oxygen $O(^1D)$ atoms from the near ultraviolet O_3 photolysis are essential quantities for atmospheric chemistry calculations because of its importance as major sources of hydroxyl (OH) radicals and nitric oxide (NO). Recently, new $O(^1D)$ quantum yields from O_3 photolysis between 230 and 305 nm in the Hartley band region were reported, which are almost independent of the photolysis wavelength (0.88–0.93) and smaller than NASA/JPL-2000 recommendations (0.95 between 240 and 300 nm). In order to assess consequences of the new data of $O(^1D)$ quantum yields on the stratospheric chemistry, the changes in stratospheric chemical partitioning and O_3 concentration are examined using a one-dimensional atmospheric model. Our steady state model simulations for 40° N in March indicate that the smaller $O(^1D)$ quantum yields result in increases of stratospheric O_3 (up to ∼2% in the upper stratosphere), which are attributed to the changes in HO_x, NO_x, and ClO_x abundance and their catalyzed O_3 loss rates.
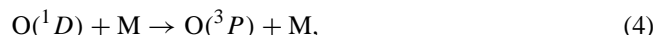
1 Introduction

Photodissociation by solar ultraviolet (UV) radiation drives much of the chemistry in the stratosphere, since it contributes to the removal of many atmospheric trace gases by decomposition and generates highly reactive radicals. One of the important photochemical reactions is the photolysis of O_3 in the UV region to produce $O(^1D)$ atoms, which react with water vapor and generate OH radicals (Brasseur et al., 1999; Finlayson-Pitts and Pitts, 1999):

$$O_3 + h\nu \rightarrow O(^1D) + O_2(^1\Delta_g), \qquad (1)$$

$$\rightarrow O(^3P) + O_2(X^3\textstyle\sum_g^-), \qquad (2)$$
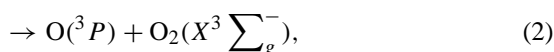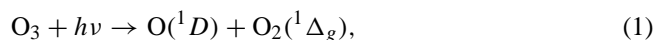
Correspondence to: N. Taniguchi
(ntanig@ics.nara-wu.ac.jp)

$$O(^1D) + H_2O \rightarrow 2OH, \qquad (3)$$

where h is Planck's constant and ν is photon frequency. The chemical reactions of $O(^1D)$ play important roles in determining the chemical composition of the stratosphere. Figure 1 illustrates the principal chemical reactions involving $O(^1D)$ in the stratosphere. Most of the $O(^1D)$ atoms produced by the photolysis of O_3 are quickly deactivated by collisions with major atmospheric species ($M = N_2$ and O_2) and then form O_3 molecules again:

$$O(^1D) + M \rightarrow O(^3P) + M, \qquad (4)$$

$$O(^3P) + O_2 + M \rightarrow O_3 + M. \qquad (5)$$

The production rate of stratospheric OH depends on the $O(^1D)$ production from O_3 photolysis. The OH radicals formed by reaction (3) initiate the HO_x catalytic cycle of O_3 loss, which is the main process for controlling O_3 loss in both the lower and upper stratosphere (Fig. 7). OH is directly involved in a HO_x catalytic cycle and also controls the partitioning between active species such as nitrogen oxides and chlorine oxides and their reservoirs:
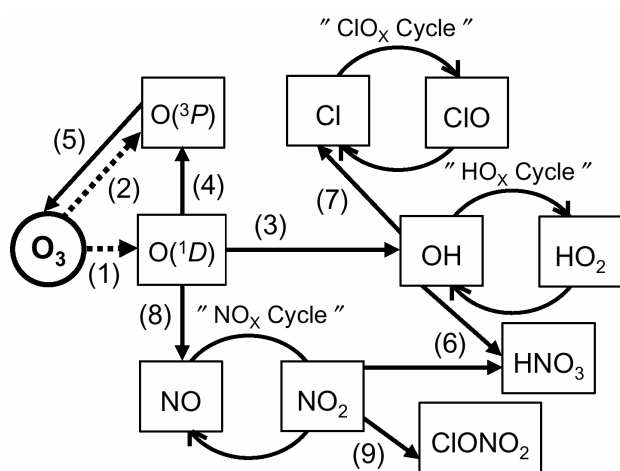
$$OH + NO_2 + M \rightarrow HNO_3 + M, \qquad (6)$$

$$OH + HCl \rightarrow Cl + H_2O. \qquad (7)$$
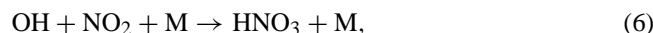
The $O(^1D)$ also produces the NO radical in the stratosphere due to the reaction with N_2O:

$$O(^1D) + N_2O \rightarrow 2NO. \qquad (8)$$

NO is the major catalyst for O_3 loss of NO_x in the middle stratosphere. NO_x also suppresses the halogen catalytic destruction of O_3 by sequestering them in unreactive forms such as $ClONO_2$:

$$NO_2 + ClO + M \rightarrow ClONO_2 + M. \qquad (9)$$
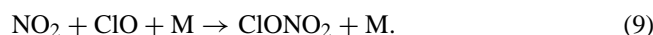
Fig. 1. Schematic of the reaction pathways involving $O(^1D)$ formation in the O_3 photolysis in the stratosphere. Dash line means a photolysis reaction. Numbers given in parentheses correspond to reaction numbers shown in the text.

The net effect on stratospheric O_3 depends on the relative contributions of these mechanisms at each altitude.

The channel branching ratios between channels (1) and (2) from O_3 photolysis have been examined extensively in the wavelength range $\lambda > 306$ nm at 298 K and low temperature by various laboratories over the past two decades (Matsumi et al., 2002, and references therein), which are used in the model calculation for such a comparison of observed and modeled OH, HO_x, and O_3 concentrations and photolysis rate of O_3 (e.g. Wennberg et al., 1999; Pfister et al., 2000). Although the O_3 chemistry of stratosphere, especially upper stratosphere, is quite simple and relatively well-understood (Brasseur et al., 1999; Finlayson-Pitts and Pitts, 1999), in the upper stratosphere and mesosphere a number of models cause an under-prediction of O_3 concentrations at 40–50 km altitude compared to observations, with magnitude of the discrepancy increasing with altitude (Eluszkiewicz and Allen, 1993). This has been known as the "ozone deficit" problem. In the upper stratosphere, the chemical composition is determined by chemical processes that are faster than the relevant dynamical processes. Crutzen et al. (1995) and Grooß et al. (1999) have investigated the O_3 budget in the upper stratosphere in comparison with observations and photochemical modeling, and kinetic reaction rate coefficients and photochemical data used in their studies were JPL-1994 and JPL-1997 recommendations for atmospheric modeling by NASA panel, respectively (DeMore et al., 1994; DeMore et al., 1997). They have pointed out that the uncertainty in the model parameters is a large source of the discrepancy although improvement of the observation quality and updated the latest model parameters decreases a significant ozone deficit. Smith et al. (2001) estimated uncertainties in model O_3 from the box model sensitivities using mecha-

nism parameter uncertainties in JPL-2000 evaluation. They reported O_3 uncertainties still remain to be near 12% in the middle and upper stratosphere and the uncertainties increase in the lower stratosphere. The JPL-2000 recommendations significantly reduced several key reaction uncertainty values, that is, O_3 catalytic photochemistry uncertainties, compared with uncertainties before JPL-2000. From the same sensitivity analysis by using JPL-1994, Dubey et al. (2000) estimated O_3 uncertainties were nearly 3–5% larger than 12% of Smith et al. (2000). Knowledge of the photochemical processes that determine stratospheric O_3 concentration is still of considerable interest. The $O(^1D)$ quantum yields in the photolysis of O_3 at wavelengths shorter than 300 nm have not received much attention and JPL-2000 panel recommended the constant value of 0.95 for the wavelength range of 240–300 nm (Sander et al., 2000). The experimental data for the $O(^1D)$ quantum yields from O_3 photolysis over the Hartley band (200–300 nm) are sparse, which may result in some notable uncertainties in the model calculation. Very recently, Taniguchi et al. (2000) and Takahashi et al. (2002) have published results of the precise $O(^1D)$ quantum yield measurements in the photolysis of O_3 between 230 and 305 nm. In this study, the atmospheric impacts of their laboratory results of $O(^1D)$ quantum yields from O_3 photolysis on the stratospheric chemistry have been explored, in the framework of a one-dimensional chemical model.

2 $O(^1D)$ quantum yield data in the photolysis of O_3

The absolute quantum yields of $O(^1D)$ formation from O_3 photolysis between 306 and 328 nm have been evaluated by Matsumi et al. (2002) with the detailed examination of recent experimental measurements as a joint activity of SPARC and IGAC. Very recently, Takahashi et al. (2002) have measured the $O(^1D)$ quantum yields from O_3 photolysis between 230 and 308 nm using a new experimental technique. Using the same technique, Taniguchi et al. (2000) have indicated that the $O(^1D)$ quantum yield in the wavelength range of 297–306 nm is almost independent of the wavelength ($\sim$0.89). In Fig. 2, the yield values presented by Taniguchi et al. (2000) and Takahashi et al. (2002) are compared with both values previously reported by other different groups (Trolier and Wiesenfeld, 1988; Cooper et al., 1993; Talukdar et al., 1997, 1998) and JPL-2000 recommendations (Sander et al., 2000). Talukdar et al. (1998) reported that the $O(^1D)$ quantum yield between 289 and 305 nm was 0.89±0.02, which is in good agreement with results presented by Taniguchi et al. (2000) and Takahashi et al. (2002). The yield values reported by Trolier and Wiesenfeld (1988) and JPL-2000 recommendations in this wavelength region are larger than values reported by Talukdar et al. (1998), Taniguchi et al. (2000), and Takahashi et al. (2002). At shorter wavelengths, JPL-2000 panel has recommended a constant value of 0.95 for the $O(^1D)$ quantum yield in the Hartley band photolysis of O_3 between
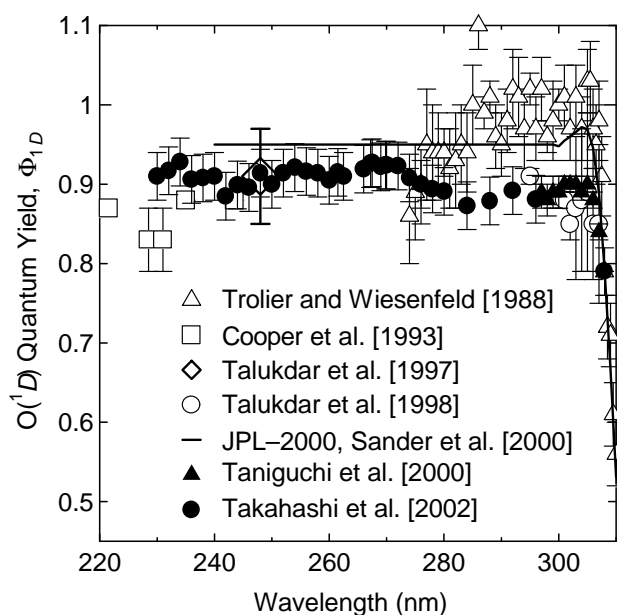
Fig. 2. The quantum yields for O(^1D) formation in the Hartley band photolysis of O_3 obtained by Taniguchi et al. (2000) and Takahashi et al. (2002). For comparison, the yield values reported by other groups are also shown (Trolier and Wiesenfeld, 1988; Cooper et al., 1993; Talukdar et al., 1997, 1998). Solid line indicates the yield values recommended by JPL-2000 evaluations for atmospheric modeling by NASA panel (Sander et al., 2000), which are constant (0.95) between 240 and 300 nm.

240 and 300 nm. The O(^1D) quantum yields presented by Takahashi et al. (2002) are almost independent of the photolysis wavelengths ($\sim$0.91) between 230 and 300 nm, which are 4$\sim$5% smaller than the JPL-2000 recommendation values and in good agreement with values determined by Cooper et al. (1993), except for 228.5 and 231 nm. Talukdar et al. (1997) reported the room temperature O(^1D) quantum yield of 0.91$\pm$0.06 at 248 nm, which is in good agreement with the value of 0.914$\pm$0.019 presented by Takahashi et al. (2002). Talukdar et al. (1998) showed that the O(^1D) quantum yields between 289 and 305 nm were independent of the temperature (203–320 K). Talukdar et al. (1997) and Takahashi et al. (1998) reported a negligible temperature dependence of O(^1D) quantum yields at 248 nm and 305 nm, respectively. We have focused on the difference in the wavelength range of 230–305 nm between the new quantum yield values (Taniguchi et al., 2000; Takahashi et al., 2002) and JPL-2000 recommendations, and examined the consequences of the difference in the chemical compositions in the mid-latitude stratosphere using a one-dimensional chemical model. The effect of the difference of the O(^1D) quantum yield values in the wavelength region of 230–305 nm should be significant in the stratosphere and very little in the troposphere, since the solar radiation at the wavelengths shorter than 305 nm mainly affects the stratospheric chemistry.
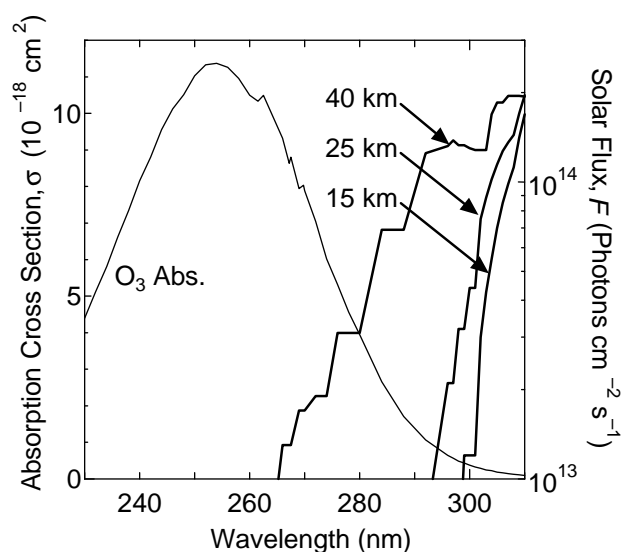
Fig. 3. Ultraviolet absorption spectrum of O_3 in the Hartley band at 263 K (Malicet et al., 1995) and actinic fluxes as a function of altitudes of 15, 25, and 40 km when the solar zenith angle is 40 degree (Finlayson-Pitts et al., 1999).

3 O(^1D) production rates in the stratosphere

The total production rates of O(^1D) atom from O_3 photolysis at several altitudes, $P_{total}(O^1D)$, were calculated by

$$P_{total}(O^1D) = \int P(\lambda)d\lambda$$
$$= \int F(\lambda)\sigma(\lambda, T)\Phi_{1D}(\lambda, T)d\lambda, \qquad (10)$$

where λ is the wavelength, and T is the temperature and F the actinic flux at the altitude. σ defines the absorption cross section of the O_3 molecule and Φ_{1D} the O(^1D) quantum yield from O_3 photolysis which is the probability for a process (1) to occur upon absorption of a photon. We calculated the $P_{total}(O^1D)$ values for the altitudes of 15, 25, and 40 km. The numerical data of F at solar zenith angle of 40 degree were taken from Finlayson-Pitts and Pitts (1999) and σ at 228 and 263 K were taken from Malicet et al. (1995) (Fig. 3). The photoabsorption cross section measurements reported by Malicet et al. (1995) are in good agreement with the recommended values by NASA/JPL 1997 and 2000 (DeMore et al., 1997; Sander et al., 2000). It should be noted that the relative O(^1D) production rate function, $P(\lambda)$, predominantly depends on the wavelength region $\sim$230–320 nm, which is limited by the sunlight spectrum penetrating into the stratosphere and by the absorption properties of O_3 molecules. Therefore, the O(^1D) quantum yield from O_3 photolysis in this wavelength region and its temperature dependence is a key input parameter for modeling calculations in the stratospheric chemistry since the predominat source of the O(^1D) atoms in the stratosphere is the photolysis of O_3. Due to the

Table 1. List of chemical species used in the one-dimensional chemical model calculations.

Initially set by Brasseur et al. (1999)					
O_3	H	OH	HO_2	H_2O_2	N
NO	NO_2	N_2O_5	HNO_4	HNO_3	H_2O
CH_4	N_2O	Cl	ClO	HOCl	$ClONO_2$
HCl	CCl_4	$CFCl_3$	CF_2Cl_2	CH_3Cl	CO

Calculated to be in steady state					
$O(^3P)$	$O(^1D)$	NO_3	Cl_2	Cl_2O_2	OClO
HBr	Br	BrO	HOBr	$BrONO_2$	CO_2
H_2	ClOO	$CHClF_2$	CH_3Br		

temperature dependence of σ and Φ_{1D}, the ambient temperature influences the O(^1D) production rate functions at each altitude. At $\lambda > 310$ nm, the O(^1D) formation via photodissociation of the vibrationally and rotationally excited O_3 and spin-forbidden process takes place (Matsumi et al., 2002). Since the population of the internally excited O_3 molecules is dependent on the temperature, the O(^1D) quantum yields at $\lambda > 310$ nm (up to ~325 nm) change as a function of the temperature (Talukdar et al., 1998; Takahashi et al., 1998; Smith et al., 2000). In the calculations for the wavelengths longer than 308 nm, the expression for the O(^1D) quantum yields recommended by JPL-2000 (Sander et al., 2000) was used, which is a function of photolysis wavelength and temperature.

We found that the total O(^1D) production rates $P_{total}(O^1D)$ estimated with the new O(^1D) quantum yields are smaller than those with the JPL-2000 recommendations by 2.5, 3.8 and 5.1%, at 15, 25 and 40 km, respectively. Atmospheric O_3 is photolyzed mainly by the UV radiation wavelength ~295–315 nm at 25 km and ~250–310 nm at 40 km, respectively. Therefore, the decreases in O(^1D) production rates caused by the new O(^1D) quantum yields in the wavelength range of 230–305 nm change the $P_{total}(O^1D)$ more effectively at 40 km than that at 25 km. Comparisons of results obtained using the smaller values of O(^1D) quantum yields with those using the recommendations of JPL-2000 clearly suggest the significance of new O(^1D) yield data. Therefore, we examined the effects of the new O(^1D) yields on the stratospheric chemistry by model calculations, as described in the following section.

4 One-dimensional atmospheric model calculations

We have examined the effect of the smaller values of O(^1D) quantum yields (Taniguchi et al., 2000; Takahashi et al., 2002) using a one-dimensional chemical model, in which all the chemical reactions related to O_3 chemistry are reasonably represented and it is suitable for assessing the impact of the new O(^1D) quantum yield data on stratospheric chemistry.

All chemical schemes in this one-dimensional model used here are the same as those used in the Garcia-Solomon two-dimensional (GS-2D) model (e.g., Solomon et al., 1996), which includes 90 kinetic reactions, 30 photolysis reactions, and 40 chemical species. Table 1 summarizes all 40 species included in this model. This one-dimensional model calculated diurnal averaged values of photolysis rates and therefore diurnal averaged mixing ratios of chemical species (by using the family method) for a specific altitude and season in mid-latitude in the northern hemisphere, by using the same formulations as those of G-S 2-D model. However, there is large difference in parameterizations of the effect of dynamics between the one-dimensional model which includes the effect of vertical diffusion and the G-S 2-D model which considers the effect of meridional transport. For the vertical eddy diffusion coefficients in the one-dimensional model, values have been chosen to match the estimates of Chang (1974). The incident solar actinic fluxes specified at the top of atmosphere are taken from World Meteorological Organization workshop report (1985) and their atmospheric attenuation is calculated in the model. The reaction rate coefficients and the absorption cross sections are taken from NASA/JPL-1997 and -2000 recommendations (DeMore et al., 1997; Sander et al., 2000). The initial mixing ratios of 24 chemical species including O_3 are taken from reference values in March at 30° N from Brasseur et al. (1999) (Table 1). The model results of vertical distributions of the chemical species and photolysis rates calculated in the one-dimensional model used in our study are approximately in good agreement with model results of vertical distributions presented in JPL-1997 and Brasseur et al. (1999) in the same conditions of latitude, altitude, and season in the northern hemisphere. This means that all the chemical reactions related to ozone chemistry are reasonably represented in our one-dimensional model and thus the model is suitable for assessing the impact of new O(^1D) quantum yield data on stratospheric chemistry. Since model responses of chemical species due to the change in O(^1D) quantum yields represent the time-dependent propagation of infinitesimal perturbations, individual responses grow and converge on the time scale associated with that process. Therefore, calculations for all chemical species with the new values or JPL-2000 recommendations for the O(^1D) quantum yields were run long enough to ensure convergence ($\pm$0.2% in concentration of all chemical species). The vertical profiles of O_3, HNO_3, and chemical families, HO_x, ClO_x, and NO_x, for 40° N in March predicted by the model are illustrated in Fig. 4, when the new quantum yield values are used. Here, the families are defined as $HO_x = H + OH + HO_2$, $ClO_x = Cl + ClO$, and $NO_x = NO + NO_2$. The solar spectral intensity is calculated for equinox in March (the solar declination angle is zero degree).

We have estimated how model concentration results for O_3 and other chemical species are affected when a new set of model parameters, that is, the new O(^1D) quantum yields are
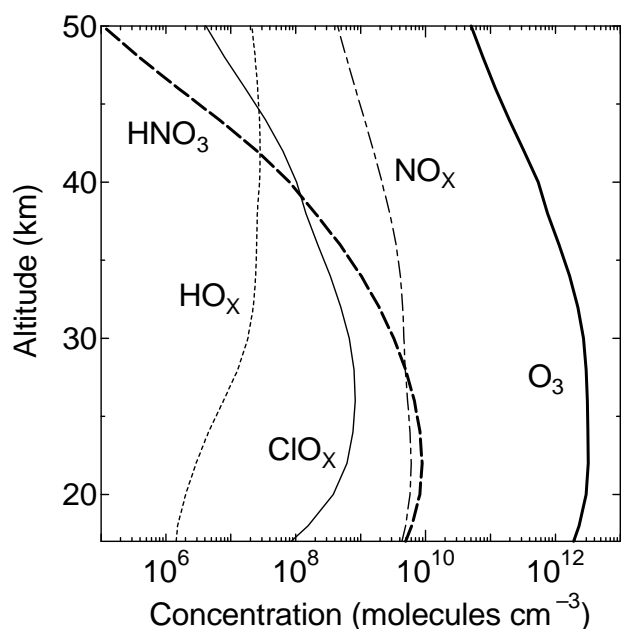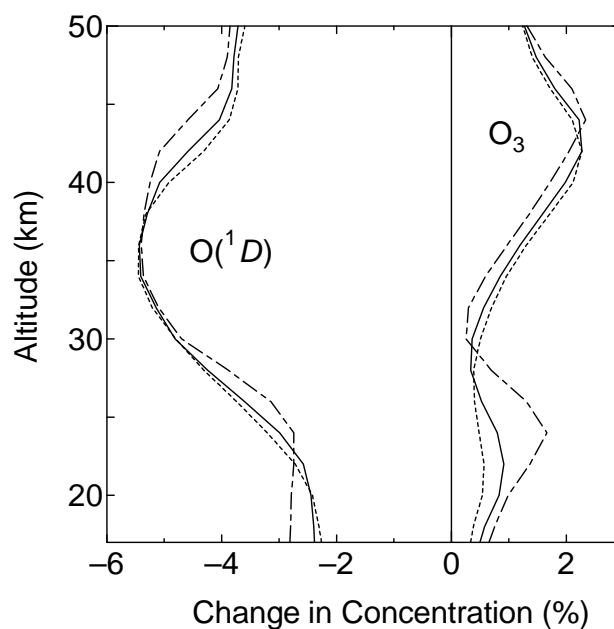
Fig. 4. Results of the one-dimensional chemical model calculations. Diurnally averaged vertical profiles of NO_x, HO_x, ClO_x, HNO_3 and O_3 (dot-dash, dot, solid, thick dash, and thick solid lines, respectively) predicted for 40° N in March using the O(^1D) quantum yield values measured by Taniguchi et al. (2000) and Takahashi et al. (2002).

Fig. 5. Results of the one-dimensional chemical model calculations. The percentage changes in diurnally averaged O(^1D) and O_3 concentrations predicted for latitude of 20, 40, and 60° N (dot, solid, and dot-dash lines, respectively) in March as a function of altitude using the O(^1D) quantum yield values measured by Taniguchi et al. (2000) and Takahashi et al. (2002), relative to those predicted using JPL-2000 recommendations for atmospheric modeling by NASA evaluation panel (Sander et al., 2000), that is, δO(^1D) and δO_3 defined by Eq. (11) in the text.

adopted. The change in O_3 concentration, δO_3, is the relative change in a predicted model concentration:

$$\delta O_3 \equiv \frac{[O_3]_{New} - [O_3]_{JPL}}{[O_3]_{JPL}} \qquad (11)$$

where $[O_3]_{New}$ is concentration of O_3 calculated with the new values of O(^1D) quantum yields from O_3 photolysis between 230 and 308 nm (Taniguchi et al., 2000; Takahashi et al., 2002), while $[O_3]_{JPL}$ is that using JPL-2000 recommendations as a standard model (Sander et al., 2000). Figure 5 shows the results of the diurnally averaged chemical model calculations, which indicates the change of the O(^1D) and O_3 concentrations, δO(^1D) and δO_3, versus altitude for 20, 40, and 60° N in March between the model runs with the new O(^1D) values and the JPL-2000 recommendations. The partitioning changes in the chemical families, NO_x, HO_x, and ClO_x, predicted as a result of the parameter changes of O(^1D) quantum yields from JPL-2000 recommendations to the new values are shown in Fig. 6.

Here, the mixing ratios of chemical species are initialized by using reference values reported by Brasseur et al. (1999) as the typical values for 30° N in March, in which mixing ratios of Cl_y are corresponded to be 0.7, 2.5, 3.2, and 3.3 ppb at 20, 30, 40, and 50 km respectively, and are in good agreement with those of WMO report (1999). Moreover, we performed sensitivity study to evaluate the impact of initial mixing ratio of Cl_y on our model results. In Fig. 5, we showed

the relative changes in the chemical concentrations calculated on the bases of the "new experimental data" and the JPL-2000 recommendations of O(^1D) quantum yields by using Cl_y initial mixing ratios from Brasseur et al. (1999). In a similar method, we calculated the relative changes in the chemical concentrations calculated on the bases of the "new experimental data" and the JPL-2000 recommendations by using the initial mixing ratios ten times as large as those of Brasseur et al. (1999). We found that there is no serious difference ($\pm0.1\%$) between the relative changes calculated with Cl_y initial mixing rations of Brasseur et al. (1999) and the relative changes with the initial mixing ratios ten times larger than Brasseur et al. (1999). These relative changes in the chemical concentrations of all 40 species included in our model (Table 1) are respectively calculated on the bases of the "new experimental data" and the JPL-2000 recommendations. In this way, we also found that that such changes in the initial mixing ratios of Cl_y as demonstrated in this sensitivity study are not likely to affect substantial influence on the evaluations of relative changes in chemical concentrations of O_3, NO_x, HO_x and ClO_x as shown in Fig. 6.

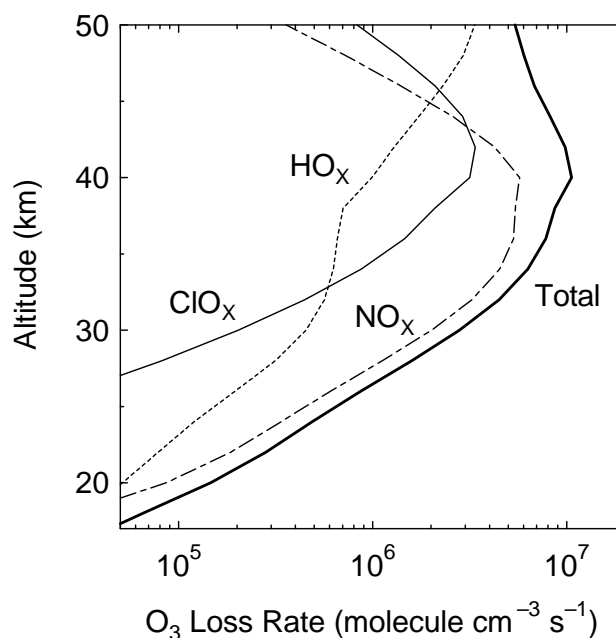Changes in the reactive families influence O_3 loss rates via the catalytic cycles involving those families. Figure 7
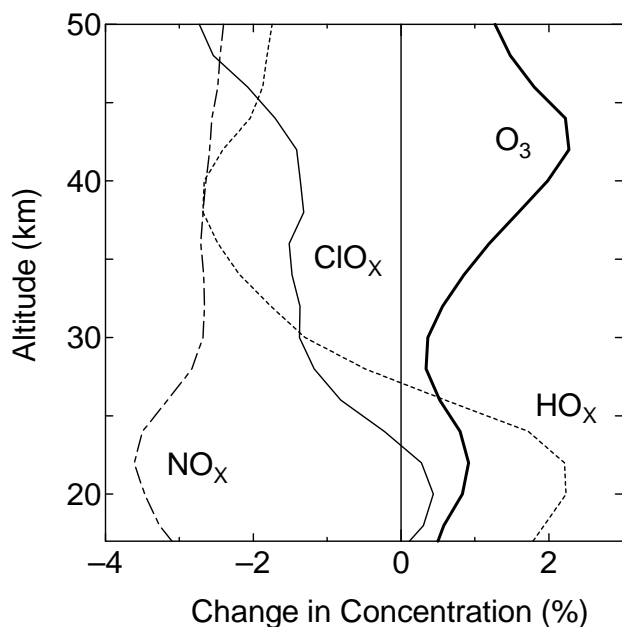
Fig. 6. Results of the one-dimensional chemical model calculations. The percentage changes in durnally averaged NO_x, HO_x, ClO_x, and O_3 concentrations (dot-dash, dot, solid, and thick lines, respectively) predicted for latitude of 40°N in March as a function of altitude using the O(^1D) quantum yield values measured by Taniguchi et al. (2000) and Takahashi et al. (2002), relative to those predicted using JPL-2000 recommendations for atmospheric modeling by NASA evaluation panel (Sander et al., 2000).

Fig. 7. Results of the one-dimensional chemical model calculations. Diurnally averaged O_3 loss rates due to NO_x, HO_x, and ClO_x chemistry (dot-dash, dot, and solid lines, respectively) predicted for latitude of 40° N in March using the O(^1D) quantum yield values measured by Taniguchi et al. (2000) and Takahashi et al. (2002). Thick line shows the total O_3 loss rate which is the sum of the O_3 loss rates in NO_x, HO_x, and ClO_x catalytic cycles.

shows the O_3 loss rates by the three principal reactive families, NO_x, HO_x, and ClO_x, versus altitude for latitude of 40° N in March, which were calculated based on the new O(^1D) quantum yield values.

5 Discussions

The steady-state O(^1D) concentration for 40° N becomes smaller by ∼2–6% with a negative peak at 35 km due to the smaller O(^1D) quantum yields from O_3 photolysis between 230 and 308 nm (Fig. 2), depending on altitude in the stratosphere as shown in Fig. 5. This result is consistent with our evaluation of the altitudinal changes in the total O(^1D) production rate P_{total}(O^1D). This indicates the consistency between the simple calculation with Eq. (10) and the one-dimensional chemical calculation, and that the concentration of O(^1D) is influenced only by the production process of O(^1D). The loss process of O(^1D) is determined by the quenching process (4) which is not affected by the changes of the concentrations of minor species in the atmosphere. The O_3 concentration calculated with the new O(^1D) quantum yields is higher than that with the JPL-2000 recommendations throughout the stratosphere. It should be noted that the change in the O(^1D) concentration influences O_3 abundance

even though atmospheric concentration of O(^1D) atoms is much lower than O_3 concentration, since the O(^1D) reactions (3) and (8) are the direct source for stratospheric HO_x and NO_x molecules which control the stratospheric radical partitioning and O_3 abundance through catalytic reactions (Fig. 1). The calculated response of O_3 concentration from these changes in the concentration of HO_x and NO_x is different between the upper, middle, and lower stratospheres because of the interdependence of the O_3 loss catalytic cycles.

As shown in Figs. 5 and 6, the absolute change in the stratospheric O_3 concentration is the largest at ∼40–45 km (increase up to ∼2%). This results from effect of the suppression of O_3 loss by the decrease of the NO_x, HO_x, and ClO_x concentrations in their catalytic O_3 loss cycles (Fig. 6). Figure 7 shows that total O_3 loss rate, that is, the sum of the O_3 loss rates in NO_x, HO_x, and ClO_x catalytic cycles has a peak around 40 km. Changes in O_3 loss rates in NO_x, HO_x, and ClO_x catalytic cycles, which were calculated from model runs with the new O(^1D) quantum yields and with the JPL-2000 recommendations, were similar to changes in NO_x, HO_x, and ClO_x concentrations which are shown in Fig. 6. Above this region, the contribution of the HO_x cycle becomes predominant drastically as the altitude increases. The HO_x concentration in the upper stratosphere is decreased by the decrease of the OH formation trough reaction (3) due

to the smaller O(^1D) quantum yield (Fig. 6). In the upper stratosphere, atomic O(^3P) constitutes efficiently the following catalytic cycle in which the rate-limiting step in the cycle is reaction (12):

$$OH + O_3 \rightarrow HO_2 + O_2, \tag{12}$$

$$HO_2 + O \rightarrow OH + O_2.$$
$$(Net : O + O_3 \rightarrow 2O_2) \tag{13}$$

Therefore, the decrease in HO$_x$ concentration in the upper stratosphere caused by the smaller O(^1D) quantum yields results in the O$_3$ concentration increase most effectively in this region. On the other hand, HO$_x$ concentration increases in the middle and lower stratosphere (Fig. 6). The NO$_x$ concentration is reduced by the decrease of the O(^1D) formation via reaction (8). This reduction of the NO$_x$ concentration takes place throughout the stratosphere. The increase of HO$_x$ concentration in the middle and lower stratosphere may be attributed to the decrease of the rate of reaction (6) due to the smaller concentration of NO$_x$. Since the contribution of three-body reaction (6) becomes more significant at lower stratospheric altitudes, HO$_x$ increases in the lower stratosphere as shown in Fig. 6.

ClO$_x$ concentration also decreases in the upper-middle stratosphere with the smaller O(^1D) quantum yields, and a little increases in the lower stratosphere. The behavior of ClO$_x$ concentration change is similar to that of HO$_x$ concentration. The chlorine reservoir compound HCl is activated to ClO$_x$ by reaction (7), that is, the reaction between OH and HCl (Fig. 1). The decreased OH production rate due to the smaller O(^1D) quantum yield results in the smaller ClO$_x$ concentration. In the lower stratosphere, the decrease of the third body reaction (9) with smaller NO$_x$ concentration may lead to the increase of ClO$_x$. ClO$_x$ cycle is important especially around 45 km and accounts for about $\sim$35% of the total O$_3$ loss rate in this region (Fig. 7).

As shown in Fig. 6, NO$_x$ concentration is decreased throughout the stratosphere by the smaller O(^1D) quantum yields, while the enhancement of O$_3$ takes place around 20–25 km (up to $\sim$1%), but slightly less around 30 km. In the middle stratosphere, the NO$_x$ catalytic cycle has the largest effect on the O$_3$ reduction (Fig. 7). The enhancements of O$_3$ concentration around 20–25 km with the new O(^1D) quantum yields should be attributed to the decrease of NO$_x$ catalytic O$_3$ loss.

6 Additional note

After submitting this paper, a new edition of the NASA/JPL evaluations has been released (Sander et al., Chemical Kinetics and Photochemical Data for Use in Atmospheric Studies, Evaluation Number 14, JPL Publication 02-25, 2003). The O(^1D) quantum yield values in the NASA/JPL-2003 recommendation have been updated from those in the NASA/JPL-2000 recommendation. The O(^1D) quantum yields from O$_3$ photolysis for $\lambda < 306$ nm are recommended to be 0.95 in JPL-2000 but to be 0.90 in the latest JPL-2003. The new laboratory O(^1D) data used in this work are in closely agreement with the NASA/JPL-2003 recommendations. Actually, we performed one-demential model calculations to compare changes in the O$_3$ concentration between the NASA/JPL-2003 recommendations and the new laboratory O(^1D) data, and the result showed very small differences in the O$_3$ concentration throughout the stratosphere ($<0.14\%$).

7 Conclusions

Consequences of the new data of O(^1D) quantum yields from O$_3$ photolysis between 230 and 305 nm in the Hartley band region on the stratospheric chemistry are examined using a one-dimensional atmospheric model. Our sensitivity studies for mid-latitude in March indicate that the smaller O(^1D) quantum yields increase the O$_3$ concentration throughout stratosphere via a decrease in the importance of NO$_x$ concentration in the middle stratosphere and the HO$_x$ in the upper stratosphere. The enhancement of O$_3$ concentration in our chemical model calculations around 40–50 km altitude by using new O(^1D) quantum yields contributes to precise assessment of the photochemical O$_3$ budget including the "ozone deficit" problem.

References

Brassuer, G. P., Orlando, J. J., and Tyndall, G. S.: Atmospheric Chemistry and Global Change, Oxford University Press, 1999.

Chang, J. S.: Simulations, perturbations, and interpretations, paper presented at 3rd Climatic Impact Assessment Program Conference, Dep. of Transp., Cambridge, Mass., 1974.

Cooper, I. A., Neill, P. J., and Wiesenfeld, J. R.: Relative quantum yield of O($^1D_2$) following ozone photolysis between 221 and 243.5 nm, J. Geophys. Res., 98, 12 795–12 800, 1993.

Crutzen, P. J., Grooß, J.-U., Brühl, C., Müller, R., and Russell III, J. M.: A Reevaluation of the Ozone Budget with HALOE UARS Data: No Evidence for the Ozone Deficit, Science, 268, 705–708, 1995.

DeMore, W. B., Sander, S. P., Golden, D. M., Hampson, R. F., Kurylo, M. J., Howard, C. J., Ravishankara, A. R., Kolb, C. E., and Molina, M. J.: Chemical Kinetics and Photochemical Data

for Use in Stratospheric Modeling, JPL Publication 94–26, JPL, Pasadena, CA, 1994.

DeMore, W. B., Sander, S. P., Golden, D. M., Hampson, R. F., Kurylo, M. J., Howard, C. J., Ravishankara, A. R., Kolb, C. E., and Molina, M. J.: Chemical Kinetics and Photochemical Data for Use in Stratospheric Modeling, JPL Publication 97-4, JPL, Pasadena, CA, 1997.

Dubey, M. K., Smith, G. P., Kinnison, D. E., Connell, P. S.: Rate Parameter Sensitivities and Uncertainties of a 2-D Stratospheric Ozone Model; LLNL Report; Lawrence Livermore National Laboratory: Livermore, CA, 2000.

Eluszkiewicz, J. and Allen, M.: A global analysis of the ozone deficit in the upper stratosphere and lower mesosphere, J. Geophys. Res., 98, 1069–1082, 1993.

Finlayson-Pitts, B. J. and Pitts Jr., J. N.: Chemistry of the Upper and Lower Atmosphere: Theory, Experiments, and Applications, Academic Press, San Diego, 1999.

Grooß, J.-U., Müller, R., Becker, G., Mckenna, D. S., and Crutzen, P. J.: The upper stratospheric ozone budget: An update of calculations based on HALOE data, J. Atmos. Chem., 34, 171–183, 1999.

Malicet, J., Daumont, D., Charbonnier, J., Parisse, C., Chakir, A., and Brion, J.: Ozone UV spectroscopy. II. Absorption cross-sections and temperature dependence, J. Atmos. Chem., 21, 263–273, 1995.

Matsumi, Y., Comes, F. J., Hancock, G., Hofzumahaus, A., Hynes, A. J., Kawasaki, M., and Ravishankara, A. R.: Quantum yields for production of O(^1D) in the ultraviolet photolysis of ozone: Recommendation based on evaluation of laboratory data, J. Geophys. Res., 107(D3), 4024, doi:10.1029/2001JD000510, 2002.

Pfister, G., Baumgartner, D., Maderbacher, R., and Putz, E.: Aircraft measurements of photolysis rate coefficients for ozone and nitrogen dioxide under cloudy conditions, Atmos. Environ., 34, 4019–4029, 2000.

Sander, S. P., Friedl, R. R., DeMore, W. B., Golden, D. M., Kurylo, M. J., Hampson, R. F., Huie, R. E., Moortgat, G. K., Ravishankara, A. R., Kolb, C. E., and Molina, M. J.: Chemical Kinetics and Photochemical Data for use in Stratospheric Modeling, JPL Publication 00-3, Evaluation Number 13, Jet Propulsion Laboratory, Pasadena, CA, 2000.

Sander, S. P., Friedl, R. R., Golden, D. M., Kurylo, M. J., Huie, R. E., Orkin, V. L., Moortgat, G. K., Ravishankara, A. R., Kolb, C. E., and Molina, M. J.: Chemical Kinetics and Photochemical Data for use in Atmospheric Studies, JPL Publication 02-25, Evaluation Number 14, Jet Propulsion Laboratory, Pasadena, CA, 2003.

Smith, G. D., Molina, L. T., and Molina, M. J.: Temperature Dependence of O(^1D) Quantum Yields from the Photolysis of Ozone between 295 and 338 nm, J. Phys. Chem., A 104, 8916–8921, 2000.

Smith, G. P., Dubey, M. K., Kinnison, D. E., and Connell, P. S.: Assessing Effects of Rate Parameter Changes on Ozone Models Using Sensitivity Analysis, J. Phys. Chem., A 105, 1449–1455, 2001.

Solomon, S., Portmann, R. W., Garcia, R. R., Thomason, L. W., Poole, L. R., and McCormick, M. P.: The role of aerosol variations in anthropogenic ozone depletion at northern midlatitudes, J. Geophys. Res., 101, 6713–6727, 1996.

Takahashi, K., Taniguchi, N., Matsumi, Y., Kawasaki, M., and Ashfold, M. N. R.: Wavelength and temperature dependence of the absolute O(^1D) production yield from the 305–329 nm photodissociation of ozone, J. Chem. Phys., 108, 7161–7172, 1998.

Takahashi, K., Hayashi, S., Matsumi, Y., Taniguchi, N., and Hayashida, S.: Quantum yields of O(^1D) formation in the photolysis of ozone between 230 and 308 nm, J. Geophys. Res., 107(D20), 4440, doi:10.1029/2001JD002048, 2002.

Talukdar, R. K., Gilles, M. K., Battin-Leclerc, F., Ravishankara, A. R., Fracheboud, J.-M., Orlando, J. J., and Tyndall, G. S.: Photolysis of ozone at 308 and 248 nm: Quantum yield of O(^1D) as a function of temperature, Geophys. Res. Lett., 24, 1091–1094, 1997.

Talukdar, R. K., Langfellow, C. A., Gilles, M. K., and Ravishankara, A. R.: Quantum yields of O(^1D) in the photolysis of ozone between 289 and 329 nm as a function of temperature, Geophys. Res. Lett., 25, 143–146, 1998.

Taniguchi, N., Takahashi, K., and Matsumi, Y.: Photodissociation of O$_3$ around 309 nm, J. Phys. Chem., A 104, 8936–8944, 2000.

Trolier, M. and Wiesenfeld, J. R.: Relative quantum yield of O($^1D_2$) following ozone photolysis between 275 and 325 nm, J. Geophys. Res., 93, 7119–7124, 1988.

Wennberg, P. O., Salawitch, R. J., Donaldson, D. J., Hanisco, T. F., Lanzendorf, E. J., Perkins, K. K., Lloyd, S. A., Vaida, V., Gao, R. S., Hintsa, E. J., Cohen, R. C., Swaetz, W. H., Kusterer, T. L., and Anderson, D. E.: Twilight observations suggest unknown sources of HO$_x$, Geophys. Res. Lett., 26, 1373–1376, 1999.

World Meteorological Organization: Global ozone research and monitoring project: Atmospheric ozone, Vol. 1, Rep. 16, Geneva, 1985.

World Meteorological Organization: Scientific Assessment of Ozone Depletion: 1998, Geneva, 1999.